E-949 TN-xxx
November 9, 2006

Experiment 949
Technical Note No. xxx

PNN2 Beam Background

Benji Lewis

Abstract

We have shown that the beam-background is much smaller that the number measured for E787-PNN2 and consistent with E949-PNN1 when phase-space is considered. We measure a total beam background of ±.

1 Introduction

The beam background analysis detailed in this technote used comis analysis that PNN1 standardized. The first step was to reproduce the results from PNN1 by using the same procedure as done in k034 section 5. We were not able to reproduce the exact number shown in k034/k038 due to changes in the pass2 source code. However, the reproduced background numbers were consistent with the k034 1/3 reported numbers to give us confidence that the current scripts and cuts were being implemented correctly. See Table 2 and 3 for the reproduced PNN1 values and Table 11 for the k034 reported values.

The working directories of the beam background is located on the TRIUMF cluster in the directory `~benjil/bmbkg/`.

Directory/Files	**Description**
./README	File describing files and how to produce results.
./src/	Source code and scripts
./backups/	Tar-ed backup of source code at various points during development.
./skim/	Output of analysis. Categorized by date.
./studies/	Additional information for specific studies.

Table 1: Beam Background Directories

1.1 Background Estimates

We measure the beam background in the standard E787/E949 bifurcation method. We assume there is at least one event remaining in all branches of the bifurcation studies, i.e. In the case of zero events remaining we change this to one.

PNN1 results shown (unless otherwise noted) are remeasured using the Spring 2006 Pass2 ntuple production requiring a pnn1 trigger and using the up-to-date set of cuts. Therefore, we expect will expect differences between the results from k034 and what is currently measured. However, with the same set of cuts, beam background in the two different kinematic regions (PNN1 and PNN2 boxes) will be a more apt comparison. The PNN2 sample results also use the ntuples from the Spring 2006 production and allowing PNN1 or PNN2 triggers. The PNN1 and PNN2 cuts differ slightly during the analysis. The following is a list of the differences.

- $K_{\pi2}$ *target scatter* cuts are not applied to the PNN1 sample.

  $K_{\pi2}$ *target scatter* cuts include the following: *chi567,verrng, chi5max, angli, ALLKfit, tpics, epionk, ccdpul, timkf.*

- For PNN2, BOX = PNN2-box (*box2.function*), layv4 = *lay_v4_pnn1.function.*

- For PNN1, BOX = PNN1-box (*boxcuts.function*), layv4 = *lay_v4_pnn1.function.*

1.1.1 ??? Boxes

Measuring the beam background at various tightness of the delayed coincidence ($DELCO$) and kinematic box cuts were attempted. Background measurement with different tightness of photon-veto (PV) was unable to be accomplished due to lack of statistics. We applied a loosened PV cut with acceptance of 95% instead of the final Photon Veto cut for this analysis. Currently we expect the final acceptance of the PV cuts to be 60%. A factor of .60/.95 = 0.63 will be used to correct the beam background measurement. We use three different DELCO cuts, *delc* (cut used by E949-PNN1), *delc or* $tpi - tk < 3$ (called *delc-3*), *delc or* $tpi - tk < 6$ (called *delc-6*). In the later cases, the event is removed if it fails *delc* or fails the $tpi - tk$ requirement. For the kinematic box, we use BOX = *box2.function* and BOX = *box2_787.function.* *box2_787* is the cut level for E787-PNN2 value and *box2* is the current kinematic box for PNN2 (more acceptance than *box2_787.*

2 1-Beam Background

The 1-beam background measurement was performed with the same cuts as E949-PNN1 adding $K_{\pi2}$ *target scatter* cuts to the normalization branch. The 1-beam background value was measured to be much smaller than the 2-beam background during early studies. Therefore, most of the work to date was concentrated on determining and lowering the 2-beam background.

The 1-beam rejection sample is tagged, as seen in Figure 1, by looking for a π-like hit at beam-time. This is done by the $b4abm\_atc < 1.0MeV$ requirement, requiring energy in the B4 detector at beam time to be π-like. The rejection sample then bifurcates. Ideally we would determine the rejection of $DELCO$ by applying the tightest constraints, $TD \cdot KIN$. However, we may loosen the cuts to improve statistics.

As shown in picture in Figure 1(b), the 1-beam normalization sample is tagged by inverting the $DELCO$ cut and applying all other cuts. In the PNN2 analysis, we also have the additional cuts from the $K_{\pi2}$ *target scatter* . DELCO unless noted otherwise refers to the *delc.function* (nominally cuts events with $tpi - tk < 2ns$) cut that was implemented in PNN1; DELCO in E787-PNN2 was $tpi - tk < 6ns$. In the PNN2 1-beam normalization branch we will define $DELCO$ as *del-6*, so that we are inverting the loosest region.

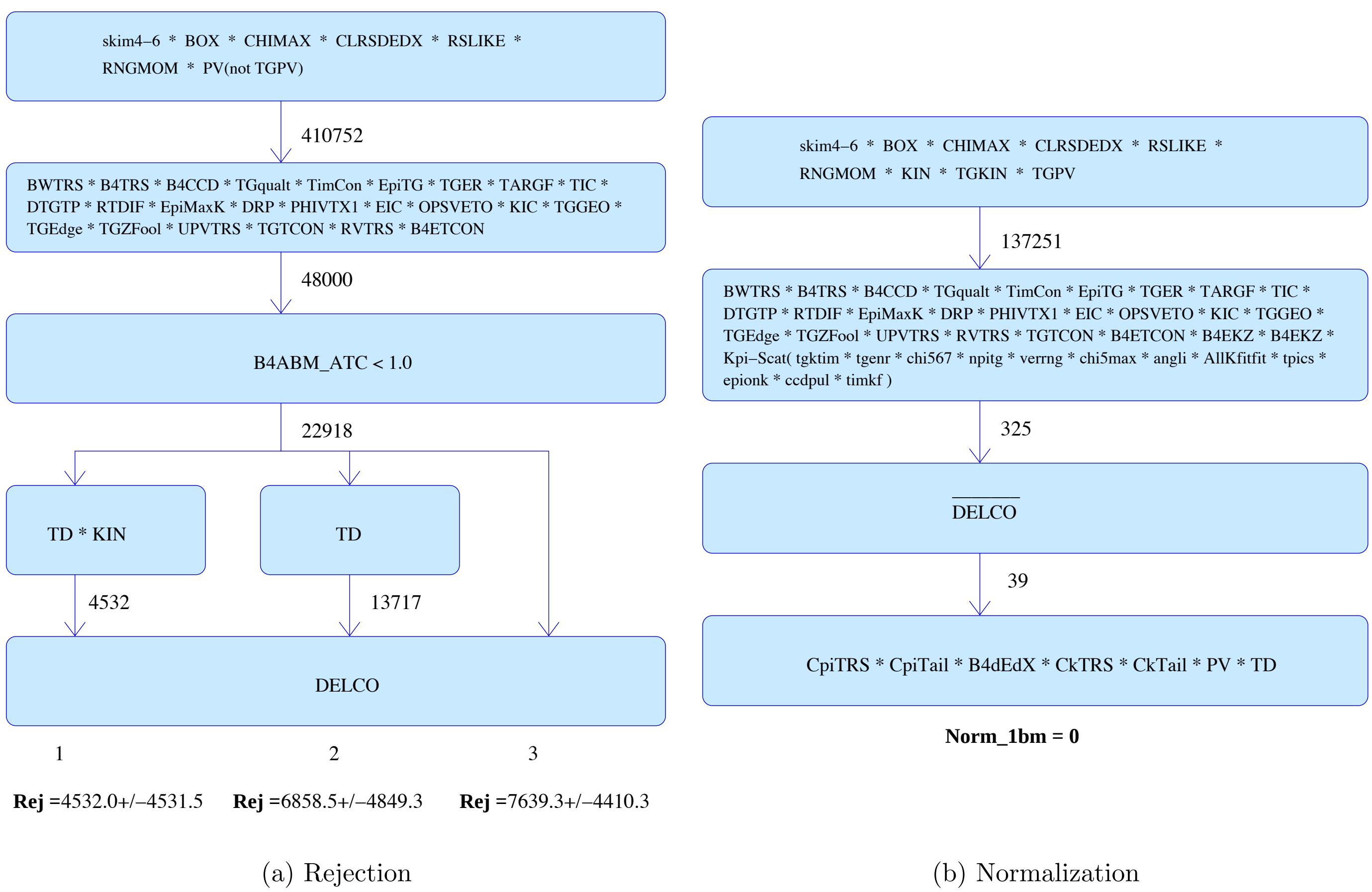

Figure 1: **1-Beam Bifurcations.** Rejection of *DELCO* is shown in (a), this cut changes depends upon the study performed, at three different levels of setup cuts. Numbers under the blue boxes are the number of events remaining after the cuts were applied. Numbers reported in this figure are for the *all runs* and DELCO=*delc*. DELCO=*delc-6* is inverted in (b).

2.1 1-Beam Results

Table 2 indicates the rejection of DELCO with different setup cuts (branches), as seen in Figure 1(a). To make a conservative estimate of the rejection, we use the minimum rejection observed in Table 2(a). After all cuts are applied, as seen in Figure 1(b), 0 events remain in the PNN2 sample (6.0 ± 2.4 events remain in the PNN1 sample). We substitute the value of 1. We now use equation 1 to determine the 1-beam background. The 1-beam background is 0.000170 ± 0.000170, as shown in Equation 4.

rejection (n)	PNN1	PNN2 (1/3)	
DELCO	*delc*	*delc,delc-3*	*delc-6*
Loose Setup	3639.8 ± 1485.8 (6)	7639.3 ± 4410.3 (3)	11459.0 ± 8102.4 (2)
TD	13451.0 ± 13450.5 (1)	6858.5 ± 4849.3 (2)	13717.0 ± 13716.5 (1)
$TD \cdot KIN$	4653.0 ± 4652.5	4532.0 ± 4531.5 (1)	4532.0 ± 4531.5 (1)

Table 2: **1-Beam (DELCO) Rejection**. These are the rejection of DELCO using the 3 branches seen in Figure 1. The first number is the rejection and the number is parenthesis is the number of events remaining in that branch. The minimum rejection is used in calculation of the 1-BM background for a conservative estimate. PNN1 column is using current level of cuts (excluding $K_{\pi 2}$ *target scatter* cuts).

Equations 1 thru 4 use measurements from the PNN2-*delc* sample with $DELCO = delc$. The factor of 3 is to scale the 1/3 data sample to the 3/3 sample. $\frac{A_{PV_{pnn2}}}{A_{PV_{beam}}}$ is the PV acceptance correction.

$$N_{1-bmbkg} = \left(3 \cdot \frac{A_{PV_{pnn2}}}{A_{PV_{beam}}}\right) \cdot \frac{Norm_{1b}}{R_{1bm} - 1} \quad (1)$$

Substitute measured quantities into equation 1.

$$N_{1-bmbkg} = \left(3 \cdot \frac{0.6}{0.95}\right) \cdot \frac{1.0 \pm 1.0}{4532.0 - 1} \quad (2)$$

$$N_{1-bmbkg} = \left(3 \cdot \frac{0.6}{0.95}\right) \cdot 0.000221 \quad (3)$$

$$N_{1-bmbkg} = 0.000418 \pm 0.000418 \quad (4)$$

$(\times 10^{-3})$	PNN1	PNN2 (1/3)	
DELCO	*delc*	*delc,delc-3*	*delc-6*
1-BM Background	4.95 ± 2.86	0.418 ± 0.418	0.418 ± 0.418

Table 3: **1-Beam Background**. Results for all tightness of *DELC* are the same.

2.2 Remaining Events

In the rejection branch, we observe one event that passes all cuts and three events that survive all cuts in the *loose setup* branch. It needs to be determined if these events are 1-beam background or contamination to the sample. After scrutinizing these three events, it is my conclusion that these events are contamination of the 1-beam background rejection sample. The conclusion is drawn from the observation of the energy and time of the kaon fibers. The reported 1-beam background is sufficiently small as to not attempt to further clean-up the contamination of the 1-beam rejection sample.

The following sections give some additional information regarding these events.

2.2.1 Run 48092 Event 92997

- Passes all 1-beam rejection cuts
- Fails: B4dEdX, B4EKZ, CHI567, TimKF
- $b4abm\_atc = 0.961877$
- $tpi - tk = 8.97$

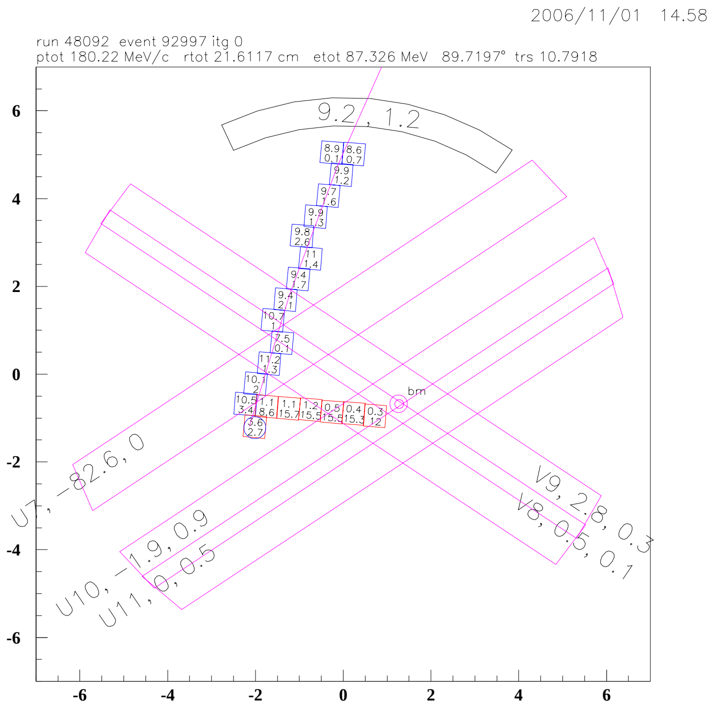

Figure 2: Run 48092 Event 92997. Red = Kaon, Blue = Pions, Green = PV. The pink curve is the UTC extrapolation. The pink blocks are B4 hits.

2.2.2 Run 50149 Event 27744

- Passes the loose setup cut branch.
- Fails: B4dEdX, B4EKZ ,CHI567, TimKF, CCDPul, TGPV, TD (via elveto), PV
- $b4abm\_atc = 0.672532$
- $tpi - tk = 21.13$

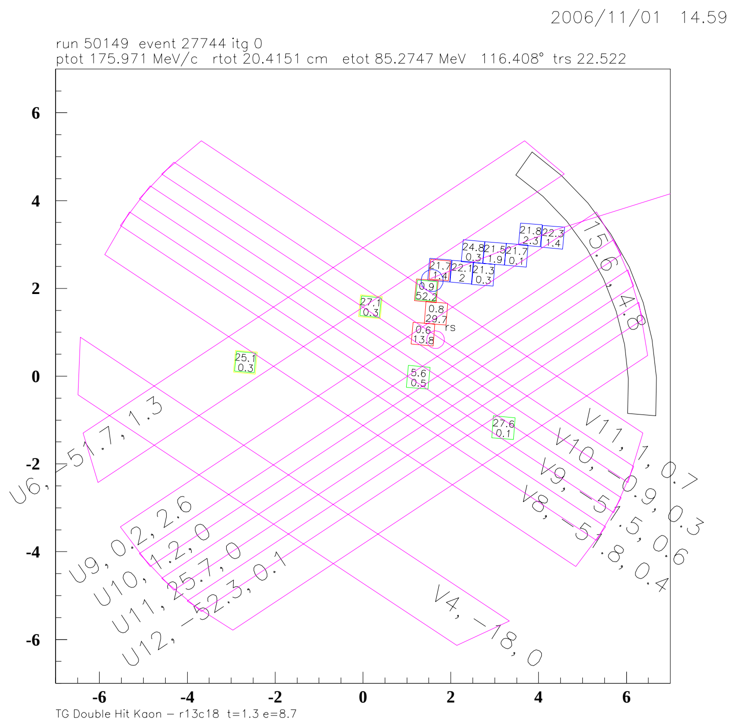

Figure 3: Run 50149 Event 27744. Red = Kaon, Blue = Pions, Green = PV. The pink curve is the UTC extrapolation. The pink blocks are B4 hits.

2.2.3 Run 47873 Event 549

- Passes the loose and the *TD* setup cut branch.
- Fails: B4dEdX, CHI567, TimKF, CCDPul, KIN (via TGDB4 and TGDB4Tip), DELCO6
- $b4abm\_atc = 0.891496$
- $tpi - tk = 4.19$

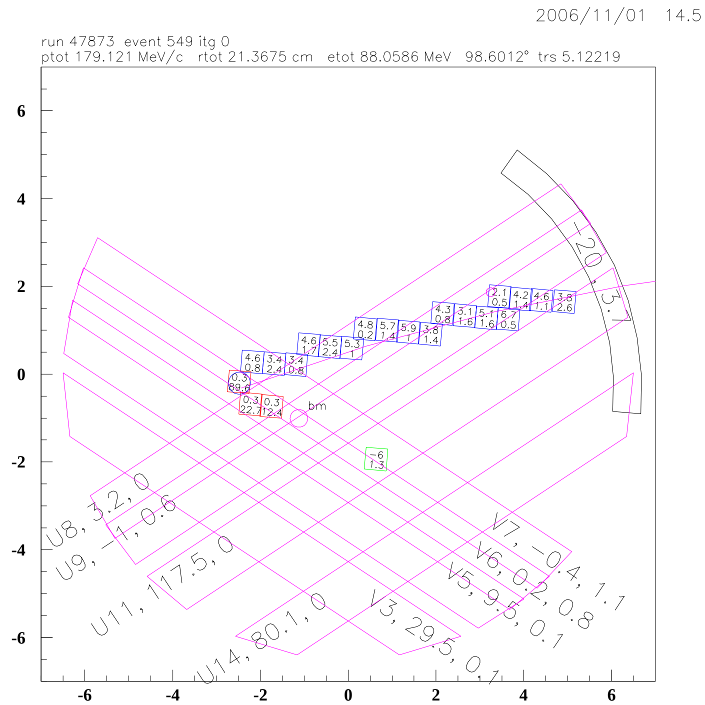

Figure 4: Run 47873 Event 549. Red = Kaon, Blue = Pions, Green = PV. The pink curve is the UTC extrapolation. The pink blocks are B4 hits.

3 2-Beam Background

It was discovered that we have an obstacle to contend with during the measurement of the 2-beam background. The obstacle is due to a PNN2 trigger definition changed after run 49151. This was documented on page 28 of k025:

- 04/29/02 19:26 49151 new pnn2 trigger pnn2_new = pnn2.and.(pnn2_ps16 $+\overline{C_\pi}$).

  The *pnn2_trigger* is
  $KB \cdot IC \cdot DC \cdot T \bullet 2 \cdot 3_{ct} \cdot 4_{ct} \cdot 5_{ct} \cdot 6_{ct} \cdot (\overline{13_{ct} + \cdots + 18_{ct}}) \cdot (\overline{19}) \cdot \overline{BV + BVL + EC} \cdot L0rr2(1) \cdot HEX \cdot L1.n$

The new trigger becomes $pnn2\_trigger \cdot (ps16 + \overline{C_\pi})$. The prescale-16 was done on the trigger board directly. A problem arises because we did not send the ps16 bit to the DAQ system. So we do not know if the trigger was from the ps16 bit or not. This effects the 2-beam Kaon-Pion (Kpi) background measurement. We do not have a large enough Kpi sample due to rejecting the Kpi events online.

There is a possibilty that we are double counting events in the 2-beam normalization branches. This is done when an event has a beam-wire (BW) hit at *trs* (track time) and does not have a hit in the Čerenkov detectors at *trs* (fail both *Cktrs* and *Cpitrs*).

Due to small statistics resulting from the trigger change, an attempt was made to increase statistics by removing $K_{\pi 2}$ *target scatter* cuts from the normalization branches. We would then apply an acceptance correction to the result. The $K_{\pi 2}$ *target scatter* acceptance loss in the E787-PNN2 analysis is 0.283. However, this method was abandoned for the scaling method, discussed in the next section.

3.1 Kaon-π (Kpi)

The trigger change required us to break the data into two sets, before and after the trigger change. With the *early runs*, runs before trigger change, (39.4% of the total KB_{Live}) we are able to proceed with the standard method done in PNN1. When we analyzed the *late runs*, runs after trigger change, we found that the statistics were very low and the background for the 2-beam Kpi was very large with large uncertainty, $N_{Kpi_{late}} = 0.1845 \pm 0.1845$ (this is the initial measurement without improvements introduced in the following sections), making the total beam-background on the same order as we were expecting from the $K_{\pi 2}$ target scattering, i.e. large enough to worry.

Since we are unable to measure the PNN2 Kpi beam-background directly we must develop an indirect way to measure the second half of the Kpi background. To analyze the 2-beam background we will first determine and understand the first half of the data. We expect that we will be able to scale the PNN1 beam background for the second half based upon the information we determine in the first half. The beam-background for PNN1 and PNN2 should only differ due to the larger phase space of PNN2. That is, we expect PNN2 to be 3 times larger than PNN1. However, the beam background for E787-PNN2 was much larger than E787-PNN1 and the difference was never understood.

As in the previous PNN2 analysis the KK dominates, so much of the work started with trying to understand and reduce this background before proceeding to the Kpi background.

As seen in Figure 5(a) the Kpi sample is tagged in a similar manner as KK. Thus the improvement (applying *kpigap* instead of $\overline{targf}$) to the KK sample also improved Kpi sample. The results can be seen in the following section.

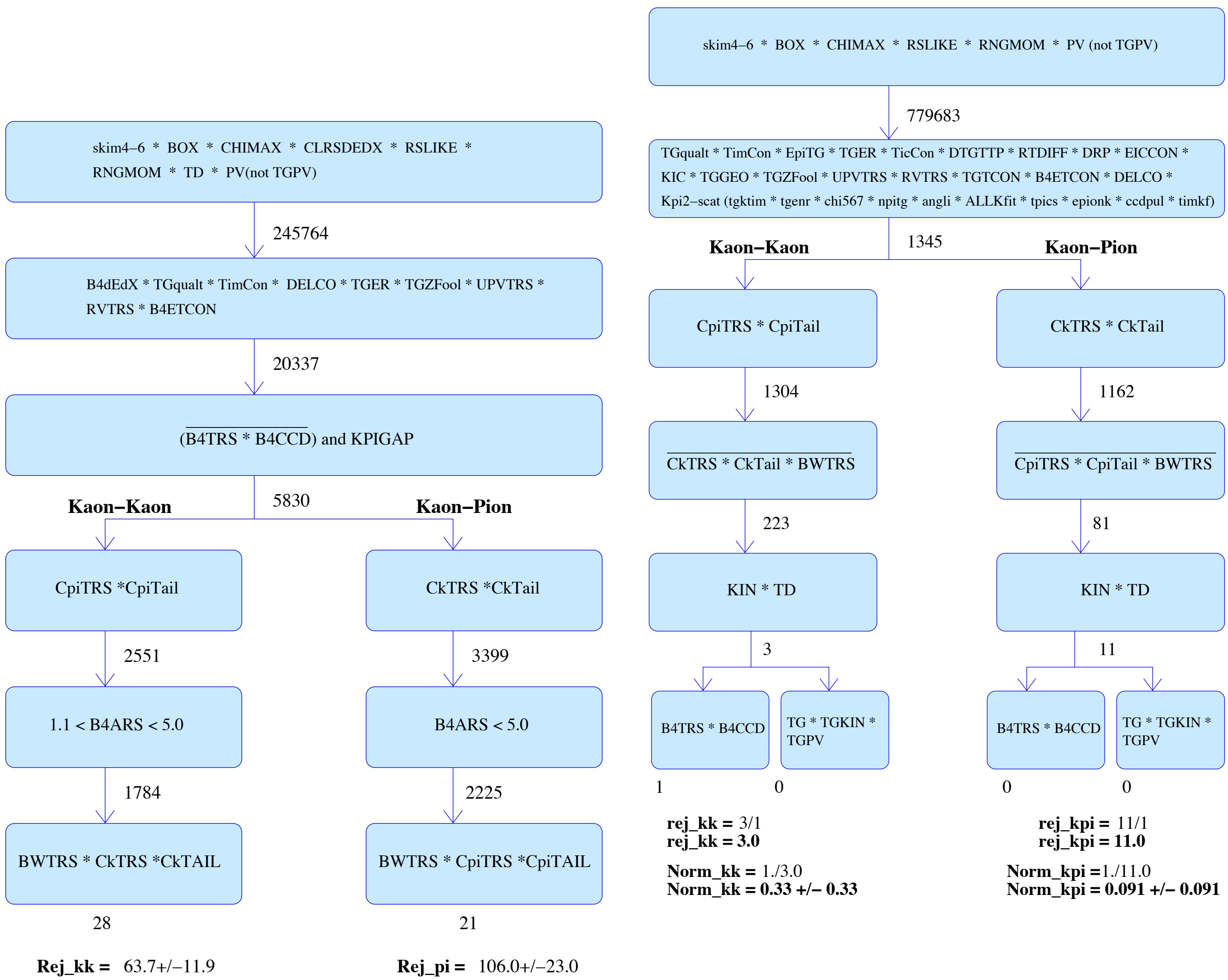

(a) Rejection

(b) Normalization

Figure 5: **2-Beam Bifurcations (Kaon-Kaon and Kaon-Pion).** *DELCO* changes depending on the study. Numbers under the blue boxes are the number of events remaining after the cuts were applied. The Kpi numbers reported in this figure are for the *early runs* and KK numbers are from *all runs*. *DELCO=delc*.

3.2 Kaon-Kaon (KK)

To measure the rejection of the 2-beam cuts we first assume that the Beam-Wire Chambers (BW) and the Čerenkov Detectors to be uncorrelated with the B4 detector. This assumption is valid because these detectors are sufficiently separated in space and the beam particles will most likely scatter in the Inactive and Active Degraders (ID/AD). So to measure the rejection of $(BWTRS \cdot CkTRS \cdot CkTail)$ we must first obtain a sample of 2-beam events, events that have two Kaons originating from upstream of the detector.

As seen in Figure 5(a), the KK rejection sample is tagged by applying $(\overline{B4TRS \cdot B4CCD} \cdot KpiGap)$. In the E949-PNN1 analysis the $KpiGap$ requirement was not in place, discussed later. The inversion of the two B4-cuts equates to having a hit in the B4 detector at Range Stack time (*trs*), so we get a 2-beam sample. We obtain a KK sample by cutting away hits that appear to be pions by applying $CpiTRS \cdot CpiTAIL$. We then require that the hit in B4 at *trs* be kaon-like by requiring the B4 energy at trs-time (*b4ars_atc*) be between 1.1 and 5.0 MeV. A pure sample of KK events exists and are now able to measure the rejection of $(BWTRS \cdot CkTRS \cdot CkTAIL)$.

In E787-PNN2, Milind and Bipul observed contamination of the 2-beam rejection sample. The contamination was from Kaon decays with multiple charged particles products like $K^+ \to \pi^+\pi^-e^+\nu$ or the $K_{\pi2} - scatter$ events with a Daltiz decay of $\pi^0 \to \gamma e^+e^-$ or conversion of photons in the target. Basically something becomes a contamination of the sample when we have something that can produce a B4 hit at decay time other than an incoming beam particle. E787 removed this contamination by adding the criteria that the tag also includes inverting the TARGF cut. So $(\overline{B4TRS \cdot B4CCD})$ becomes $(\overline{B4TRS \cdot B4CCD}\ AND\ \overline{TARGF})$. TARGF removes events when the minimum distance from any kaon fiber to any pion fiber in the Target (from fiber center to fiber center) is greater than 0.7, i.e. will cut any event when the kaon and pion fibers are not adjacent. This essentially removes any events that have a decay product emerging from the Kaon identified by *swathccd* . We make an assumption here that the 2-beam background is the same whether the two particles come close geometrically in the target or are separated.

KK events remaining Figure 5(a) is 28, the final result. When one applies $\overline{targf}$as was done in E787-PNN2, instead of *kpigap* for the 1/3 *early runs*. The rejection is measured to be very low, 29.6 ± 3.8. A visual scan of these 58 remaining events was performed to determine what if any contamination we have.

After scanning most of the 58 events it was evident that around a half of the events were due to target scatters, which is PNN2's largest background. As seen in Figure 6, *swathccd* was unable to correctly reconstruct this event. However, visually we are able to easily discern that the photon-veto fibers adjacent to the kaon fibers are in fact pion fibers before a scatter occurred in the 18.2 MeV fiber. These scatter events were tagged because the products from the decay caused hits in the B4 detector, i.e. not from a second beam particle. This discovery led to the creation of a modified version of $\overline{TARGF}$, *kpi_gap* .

3.2.1 *kpi_gap* cut

The signatures of a TG-scattering event that is reconstructed (incorrectly) by *swathccd* are photon-veto fibers adjacent to the decay vertex and the photon-veto fibers being between the pion fibers and the decay vertex. A better and complete method would be to incorporate the *TGrecon* and *KinkFinder* . However, this solution requires reprocessing of the data at the PASS2 level and extensive coding. A very basic and quick solution was formed by creating a comis function that was named *kpi_gap.function* and placed in the `$PASS2_ANAL/func/` area.

kpi_gap has the following coding steps.

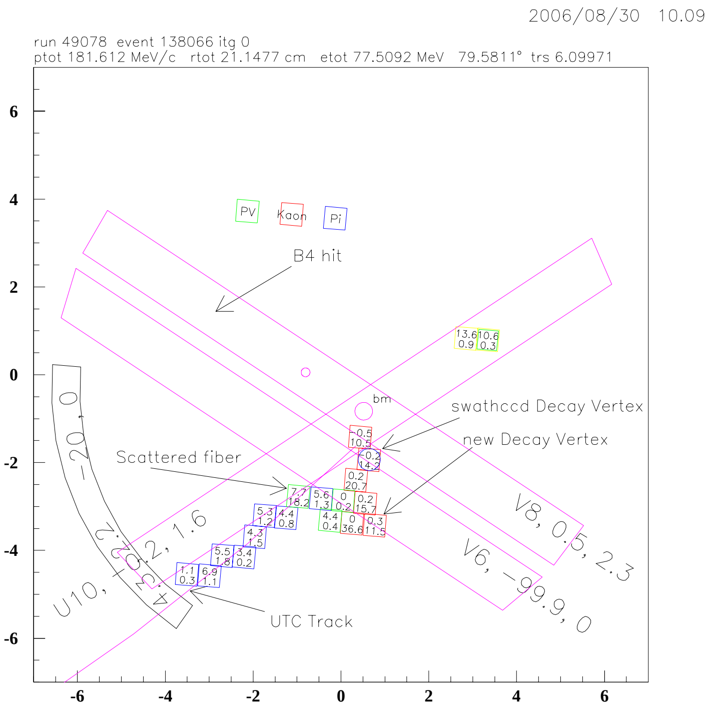

Figure 6: Example of a Scatter event that will be removed by *kpi_gap* . Red = Kaon, Blue = Pions, Green = PV. The pink curve is the UTC extrapolation. The pink blocks are B4 hits.

- $\overline{TARGF}$
- Search for PV-fibers that are within $\pm 3ns$ of *trs* and adjacent to a kaon fiber (within 0.7cm center to center). Let's call these PV' fibers. If no PV' exist, then the event passes *kpigap* and can remain in the 2-beam rejection sample.
- If a PV' fiber is adjacent to *swathccd*'s determined decay vertex, then remove event from the sample (fails cut).
- Determine the best decay vertex with the given information.

  Modified *decay_vertex.function* to determine the decay vertex based upon B4 information (if available). If B4 information is not available, then default to *swathccd* 's determination (tgx,tgy). An example of the determination of a new Decay Vertex is shown in Figure 6.
- Determine if one of the PV' fibers are within a box. The determined decay vertex is one corner and the nearest (*swathccd* determined) pion is the other corner. This step forces the photon-veto fiber to be between the pions and the decay vertex. This also helps when the decay-vertex finder, previous step, isn't able to determine the best fiber, i.e. gets close but not exact.
- Because the previous step's "box" could have very little area if the decay vertex and pion fiber are on the same row of the target, we will also search for any PV' fibers that are within 1.02 cm of the decay vertex (close to the decay vertex, but still adjacent to a kaon fiber).

The end result is that *kpi_gap* is a tighter version of $\overline{TARGF}$, such that *kpi_gap* $\approx \overline{TARGF}\cdot$(cut events with in time PV fibers near decay vertex). With this new tool, the 58 events were scanned and classified. Table 4 shows a quick breakdown on how the events were classified. Figure 7, shows the *tgz* distribution of events analyzed in Table 4. A detailed discussion about the KIC event and the remaining kink event (contamination) are located in the sections that follow.

Type	**# of events**	**Comments**
bad run	1	BWPC off
kpi_gap	23	23 of 23 are kinks or non 2-beam events.
+*tgzfool*	22	Events that pass *kpi_gap* , but fail $tgz < -5$.
kinks	1	Did not get removed by *kpi_gap* .
KIC	1	2-beam event where one particle emerges from the Range Stack.
unknown	2	Most likely 2-beam, but not very clear.
2-beam	8	Does not include ones removed by *tgzfool*/*kpi_gap*
Total	58	

Table 4: Classification of events that survive the initial 2-beam KK rejection cuts (tagging with $\overline{TARGF}$. In the 1/3 PNN1+PNN2 sample before the PNN2 trigger change.

- The 'bad run' event was due to the beam-wire chambers being off. Further details about this event is located in the *Addition to the Bad Run List* technote.

- 22 of 23 events found by *kpi_gap* are TG-scatters. The remaining event is difficult to classify, but possibility a kink. However, this event is not a 2-beam event. So over 40% of the previous events that pass all cuts in the KK-rejection sample were contamination. Using *kpi_gap* removes most of the TG-scattering contamination.

- 22 events passed *kpi_gap* but failed the cut $tgz < -5.cm$, which is the E787-PNN2 cut E949-PNN1 had the *tgzfool* cut set at -15.0cm. We are implementing this cut to remove pions that scatter in the B4. Also, we do not want to accept events where the pions come from outside the TG.

- 1 TG-scattered event was not removed by *kpi_gap* . This event is discussed in detail a later. This event is considered contamination to our tagged sample.

- 11 events are 2-beam, this includes the one KIC event and the 2 unknowns.

- 12 total beam candidates exist.

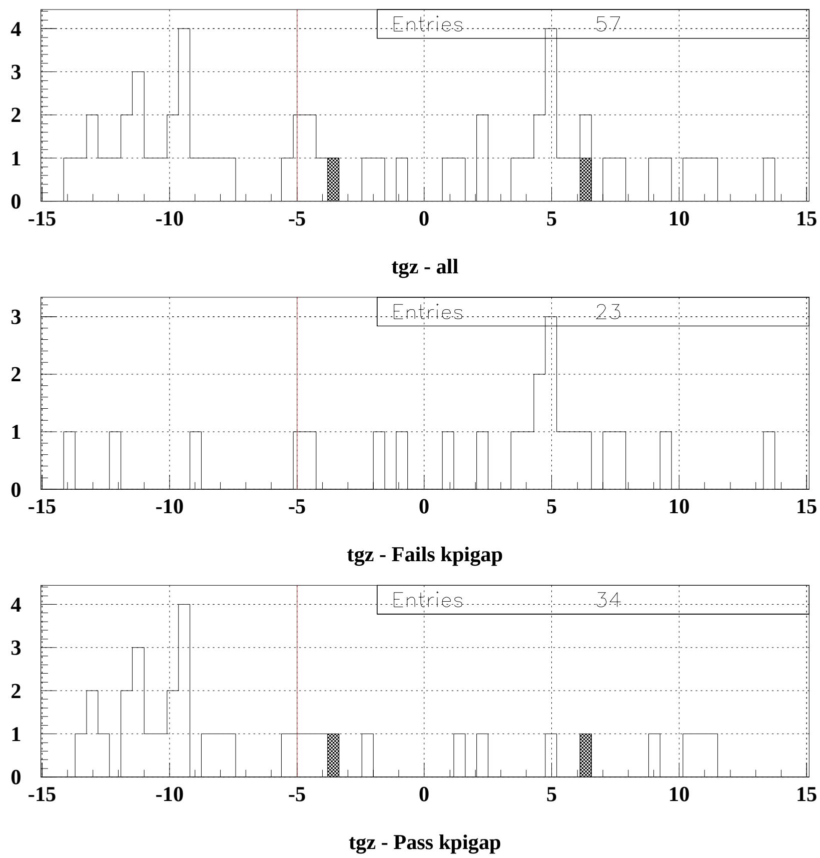

Figure 7: *tgz* **plots.** The top plot shows all 57 events examined (the *bad run* event is omitted) in the KK rejection study. The middle plot shows the tgz values of the events that fail *kpigap* and the bottom plot show the events that are tagged by *kpigap*. The red line is the E787-PNN2 threshold for *tgz*, remove events $< -5.0cm$. The KIC event and the kinked event that *kpigap* failed to remove are shaded, -3.5cm and 6.2 cm respectively.

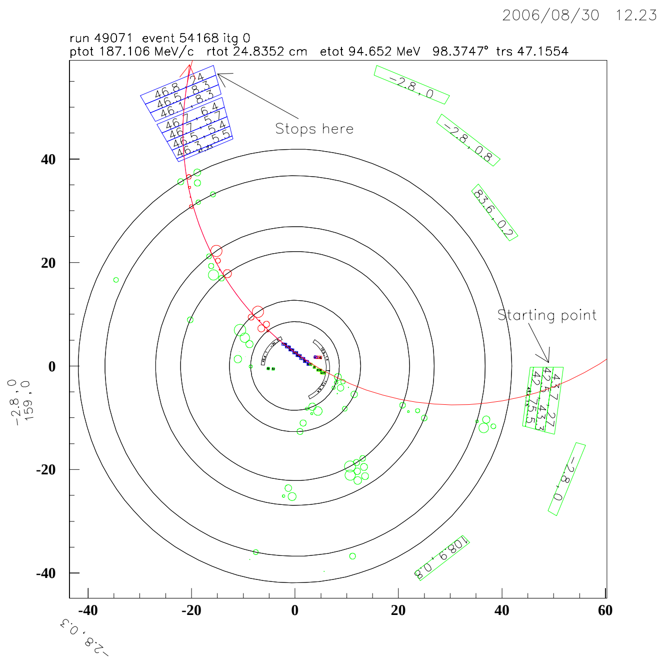

(a) xy-view

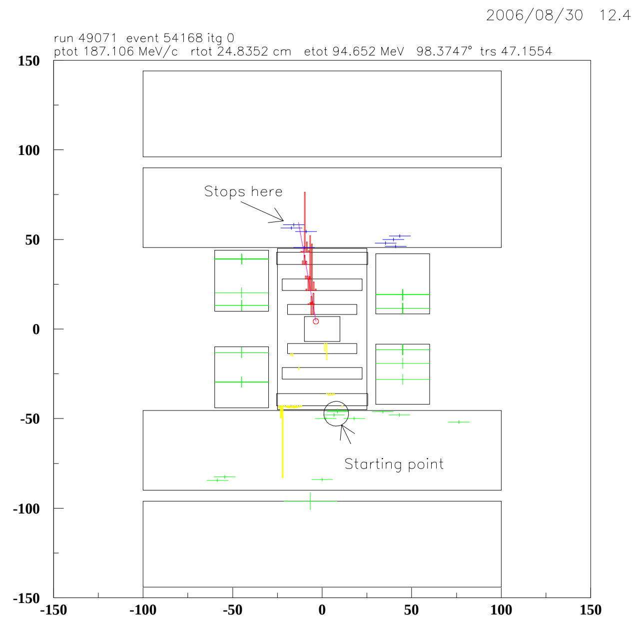

(b) z-view

Figure 8: KIC Event. The red curve is the UTC extrapolation.

3.2.2 KIC event

The pion track in event 54168 run 49071 starts in the Range Stack (RS) and passes thru the Target (TG) and creates the $T \bullet 2$ trigger on opposite side of the RS as seen in Figures 8(a) and 8(b). The initial hits in the RS occur at $t \sim 43.ns$ and the time of the $T \bullet 2$ trigger is $\sim 47.ns$. This is a difference of $\sim 4.ns$ which is the time it takes to traverse the UTC chamber distance. We have to manually determine the total energy and range, due to the incorrect reconstruction. $E_{total} \geq 102.MeV$ there is an unknown amount of energy in the initial RS-cluster. $R_{total} \approx 29.cm$. The total range and energy is consistent with a $K_{\pi 2}$ decay. This would indicate that an initial Kaon at $t \sim 0.ns$ stopped in the TG and then another Kaon entered the RS detector at $\sim 43.0ns$ and promptly decays. The π^+ traverses the UTC and TG and comes to rest in the RS on the other side of the detector.

There are 14 hits at 43.ns (-4.17ns relative to *trs*) in the Čerenkov counter. CKTRS (*ckt_rs.function*) basically cuts the event if we have 5 or more hits within 2ns of *trs*. Since the second K^+ enters 4ns before the $T \bullet 2$ trigger CKTRS does not remove this event. This suggest that we may need to create a cut to remove events of this type. This cut would remove events with the following properties:

- Large energy in the inner layers of the Range Stack (RS) before *trs* (possibliy a window around $trs - 4$) on the opposite side of the RS.
- The I-Counter (IC) photon veto cut would also be useful in cutting KIC-type events.
- A certain number kaon Čerenkov counters which have hits at $\sim 4ns$ before *trs*, *cktrs* requires 5 counters have hits within a time window of $2ns$.

I believe a study is needed to investigate whether we need to create a cut to remove KIC-type events. At minimum a safety cut should be in place.

We also see the second K^+ in both BW chambers. The K^+ is not observed in the Active Degrader (AD). So we must assume that the K^+ somehow scatters into the RS after BW-2 and before the AD. So this event is a 2-beam KK event since the second K seems to initially come from the beamline and then scatters into the fiducial region. However, the B4 hit that flags this event is only located in one plane (U10) of the B4. There are two hits in element U10. One hit at -1.0ns and another at 44.98ns both have a recorded energy of 1.47019MeV (note that the B4 energy cut in the KK branch is [1.1,5.0]). The energies of the two hits are identical. The CCD channel was unable to discern the second hit and so both hits are given the same energy. So the true energy of the second hit, which causes the flag, could be very small.

3.2.3 Remaining kink event

Only one event of the 58 that was identified visually as a TG-scatter (kink) and was unable to be removed by *kpi_gap* , event 129159 run 48435. This events shows a possible loophole in the analysis that needs to be carefully investigated. The loophole is when the second beam particle comes into the detector between beam-time and *trs*.

The following description of the event goes along with Figure 9.

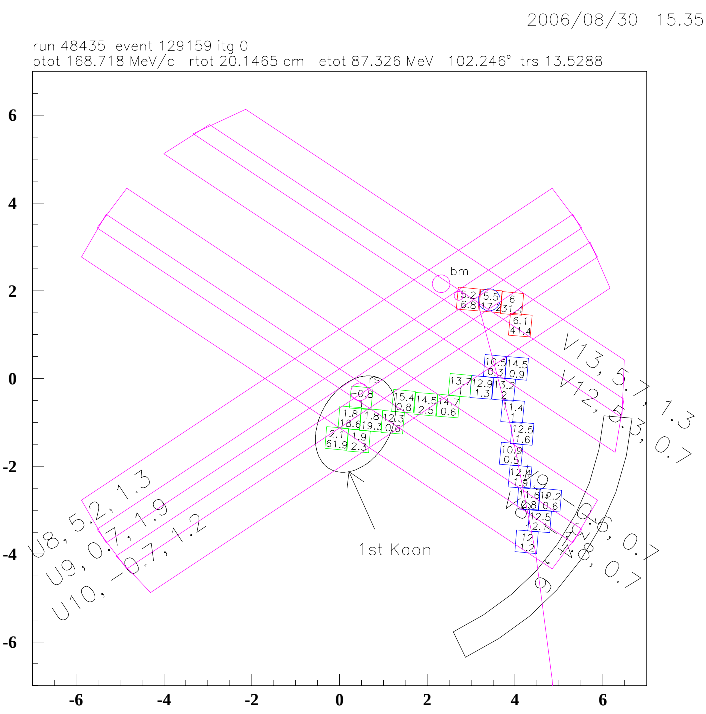

Figure 9: View of the TG with the B4 detector overlayed. Kinked event which *kpi_gap* is unable to remove from sample.

- The first Kaon enters at time$\sim 0ns$ TG and is observed by the B4 detector and TG.

- A second Kaon enters the TG and is observed by the B4 detector at $\sim 5.5ns$. Because the second K^+ is within the swath *swathccd* identifies it as the initial Kaon.

- The first K^+ decays at $\sim 13ns$ travels over 4cm in the target and scatters and ultimatily creates the $T \bullet 2$ trigger.

- $\overline{b4ccd}$ is what flags this event for the 2-beam rejection sample. This lead to an investigation of the *b4ccd* cut. See following section which gives further details.

- A hit with 133 counts ($\sim 21.MeV$) in the AD at *trs*.

- This event fails *ccdpul*. The ccdfiber observes 2MeV around 16ns. This could possibly be some type of conversion of the first K^+'s decay.

3.2.4 *b4ccd.function*

The *b4ccd.function* used during the PNN1 analysis had a problem with the algorithm's clustering of hits in the same plane. The algorithm would only add a hit to the cluster if it was in time and adjacent to the first hit in the cluster. The correct method would allow a hit adjacent to any element in the cluster. The PNN1 method would be dependent on the original ordering of the hits in the element. The error has been corrected. No additional events were observed in the KK 2-beam rejection branch after the correction.

Another potential problem is 'averaging' the total area of the cluster's pulse. This does not seem correct to do this. However, the cut requires a minimum of 500 units of total energy and this could have been optimized using the 'average' pulse area.

3.2.5 A look at a prime $K_{\pi 2}$-scatter event.

The reader can skip this section because it is of little importance to the 2-beam background. It is included here because this event was observed in the 2-beam KK rejection study and is an ideal example of a $K_{\pi 2}$ $target\ scatter$, the largest background in PNN2.

Event 34104 run 49037 is no longer tagged in the 2-beam KK rejection sample due to *kpi_gap* not allowing PV fibers adjacent to the Kaon fibers. We can reconstruct the event as follows:

- Incoming K creates hits in all beam detectors (B4 and TG hits seen in Figure 10(a)) and comes to rest after 92MeV in the TG.

- In Figure 10(b) you can see the that there are very high-energy fibers in time with *trs* in the kaon fibers.

- We know that the particle emerging from the Kaon is traveling upstream because we see the UTC track extrapolate into the B4 counter in Figure 11. The Pion scatters in B4 into the fiducial region and creates a false tag in the B4 at *trs* (removed by requiring *kpi_gap*).

- The Pion traverses the edge of the TG to give some pion hits in the TG, which is required in PNN2.

- We observe a photon conversion in the TG in Figure 10(b). The TG is able to contain the entire energy of the photon since the photon is traveling in the downstream z-direction, opposite the Pion.

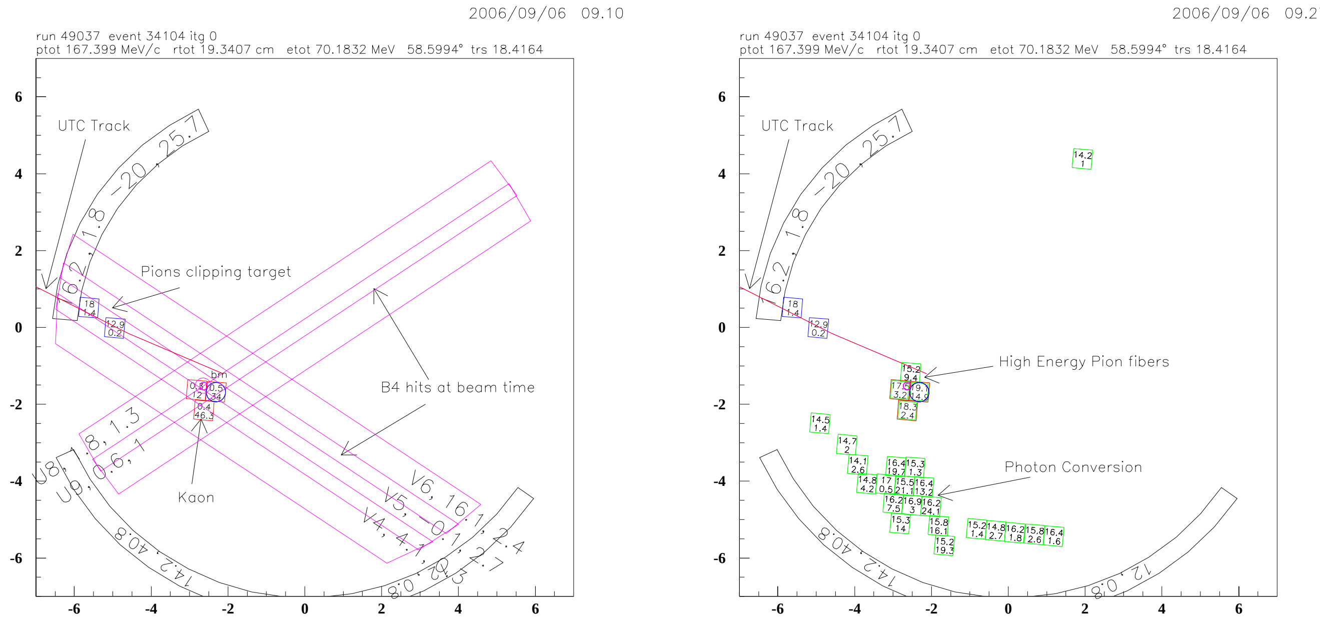

(a) Kaon and Pions in Target

(b) z-going Pions and Photons in Target

Figure 10: Run 49037 event 34104. An example of a $K_{\pi 2}$ *target scatter* .

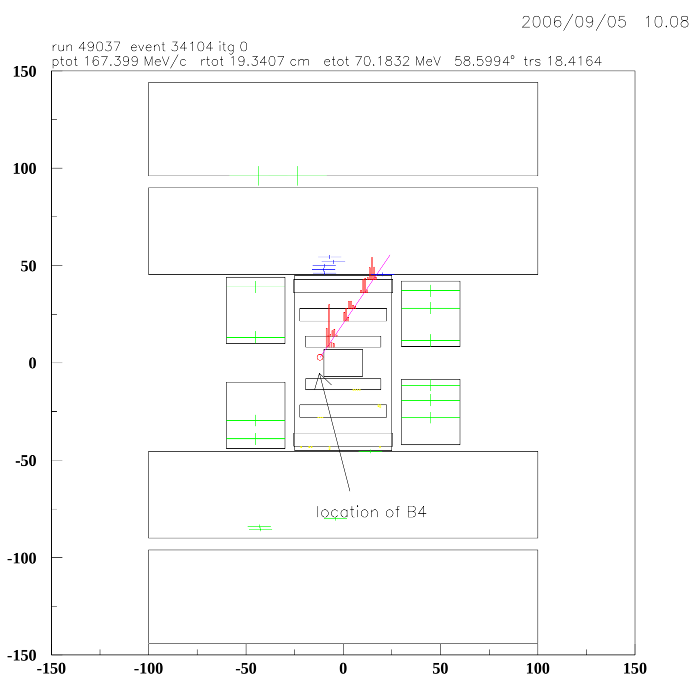

Figure 11: Z-View of Run 49037 event 34104. The orgin of the π is in the B4-counter (outside of the target. Also, note that the UTC track clips the edge of the target which we see in Figure 10 in the form of 2 pion fibers.

3.3 2-Beam Background Estimate

Tables 5 and 8 show the KK and Kpi rejection seen in Figure 5(a). Tables 6 and 9 show the result from the KK and Kpi normalization seen in Figure 5(b). Tables 5 thru 7 use the PNN1 sample. The columns in the tables are $run \leq 49151$ (early runs), $run > 49151$ (late runs), and *All Runs*. The three run ranges were done to compare effects from the PNN2 trigger change at run 49151. In the *late runs* columns for PNN2 data we require a $\overline{C_\pi}$ ($ext(16) = true$ is cut) and in the *All Runs* we require a $\overline{C_\pi}$ when $run > 49151$. We have no such $\overline{C_\pi}$ requirement for PNN1 data.

We intend to scale N_{Kpi} for PNN2 data for the early runs by $f_{PNN1} = \frac{N_{Kpi_{late}}}{N_{Kpi_{early}}}$ from the PNN1 data, seen in Table 7. This scaling factor is $\frac{0.03}{0.15} = 0.2$. The factor is less than 1 due to additional statistics observed in the set of late runs. This is due to the increase in R_{Kpi}, see Table 5, 7154.0 for the *late runs* and 2020.0 for the *early runs*.

We expect 1.53 times more background in the late runs because we have more KB_{Live} in the late runs as compared to the early runs. Scaling by f_{PNN1} seem unrealistic, since we would obtain a smaller central value for a larger set of the data. Hence, we must determine another method for to determine $N_{Kpi_{late}}$ for the PNN2 data. We have $KB_{Live_{all}} = 1.714 \times 10^{12}$ and $KB_{Live_{\leq 49151}} = 6.7507 \times 10^{11}$ (39.4% of KB_{Live} in early runs and 60.6% in the late runs). A possible method to determine N_{Kpi} is to scale by the amount of KB_{Live} in the respective data sets. The scaling factor is $f_{KB_{Live}} = \frac{.606}{.394} = 1.54$.

This measurement gains validity by observing in Tables 7 that N_{Kpi} for PNN1 triggers is consistent for the early and late runs. Also, in Table 10, N_{KK} is consistent for PNN2 data in the early and late runs. Everything indicates that we did not have an increase in beam background after the trigger change occurred. Therefore, scaling by $f_{KB_{Live}}$ is valid. The result of the scaling is shown in Table 10. Scaling by KB_{Live} yields $N_{Kpi}^{scaled} = 0.00142 \pm 0.00142$ which is consistent with the direct measurement, $N_{Kpi}^{direct} = 0.00164 \pm 0.00164$. We measure N_{Kpi} directly by omitting PNN2 triggers that do not have a $\overline{C_\pi}$ after run 49151. The early runs have a larger weight on the N_{Kpi}^{direct} result because of the lack of statistics in the later runs. Hence, the final N_{Kpi} will be determined by the results from the KB_{Live} scaling. The 2-beam results are summarized in Table 10, where the bold values are the numbers used to determine the final N_{Kpi} measurement.

$rejection\ (n)$	$\leq run$ 49151	$> run$ 49151	All Runs
$R_{KK}:\ BWTRS \cdot CkTRS \cdot CkTail$	75.0 ± 74.5 (1)	152.0 ± 151.5 (1)	113.5 ± 79.9 (2)
$R_{Kpi}:\ BWTRS \cdot CpiTRS \cdot CpiTail$	2020.0 ± 2019.5 (1)	7154.0 ± 7153.5 (1)	9174.0 ± 9173.5 (1)

Table 5: **PNN1 2-Beam Rejection**. First number is the rejection and the number in parenthesis is the number of events remaining. The sample is PNN1 triggers with *boxcuts* (pnn1box), *lay_v4_pnn1*.

$Norm.\ branches$	$\leq run$ 49151	$> run$ 49151	All Runs
$n_{KK}:\ B4TRS \cdot B4CCD$	1.0 ± 1.0	1.0 ± 1.0	1.0 ± 1.0
$r_{KK}:\ TG \cdot TGKIN \cdot TGPV$	16.0 ± 15.5	16.0 ± 15.5	32.0 ± 31.5
$Norm_{KK} = \frac{n_{KK}}{r_{KK}}$	0.0625 ± 0.0625	0.0625 ± 0.0625	0.0313 ± 0.0313
$n_{Kpi}:\ B4TRS \cdot B4CCD$	10.0 ± 3.2	55.0 ± 7.4	65.0 ± 8.1
$r_{Kpi}:\ TG \cdot TGKIN \cdot TGPV$	97.4 ± 43.3	815.5 ± 576.3	302.6 ± 114.2
$Norm_{Kpi} = \frac{n_{Kpi}}{r_{Kpi}}$	0.103 ± 0.004	0.067 ± 0.002	0.215 ± 0.085

Table 6: **PNN1 2-Beam Normalization**. The 2-BM Normalization has 2 branches that are further bifurcated as seen in Figure 5(b). The results of all 4 branches are shown in $n_{Kpi,KK} r_{Kpi,KK}$. The normalization results are in the $Norm_{KK,Kpi}$ rows.

$Bkgrnd$ ($\times 10^{-3}$)	$\leq run$ 49151	$> run$ 49151	All Runs
2-BM KK	2.50 ± 2.50	1.23 ± 1.23	0.83 ± 0.83
2-BM Kpi	0.15 ± 0.15	0.03 ± 0.03	0.07 ± 0.07
2-BM	2.65 ± 2.65	1.26 ± 1.26	0.90 ± 0.90

Table 7: **PNN1 2-Beam Background.** Scaled to the 3/3 sample. The errors are statistical.

	$\leq run$ 49151 *delc*, *delc-3*	$\leq run$ 49151 *del-6*	$> run$ 49151 *delc*	All Runs *delc* and *delc-3*	All Runs *delc-6*
R_{KK}	43.6 ± 12.0 (13)	46.9 ± 13.4 (12)	81.1 ± 20.8 (15)	63.7 ± 11.9 (28)	65.3 ± 12.5 (27)
R_{Kpi}	339.0 ± 138.2 (6)	336.5 ± 137.2 (6)	12.7 ± 3.2 (15)	106.0 ± 23.0 (21)	105.1 ± 22.8 (21)

Table 8: **PNN2 2-Beam Rejection**. Shown are the KK and Kpi rejections, as seen in Figure 5(a). R_{KK} is the rejection of $BWTRS \cdot CkTRS \cdot CkTail$ and R_{Kpi} is the rejection of $BWTRS \cdot CpiTRS \cdot CpiTail$. Also, shown are rejections with different tightness of *DELCO*, *delc*, *delc-3*, and *delc-6*. $> run$ 49151 is only done for *delc* since we are using the scaling method. Numbers in parenthesis are the event remaining used to calculate the rejection.

Norm. branches	$\leq run$ 49151 *delc*, *delc-3*, *delc-6*	$> run$ 49151 *delc*	All Runs *delc* and *delc-3*	All Runs *delc-6*
$n_{KK}:\ B4TRS \cdot B4CCD$	1.0 ± 1.0	1.0 ± 1.0	1.0 ± 1.0	1.0 ± 1.0
$r_{KK}:\ TG \cdot TGKIN \cdot TGPV$	2.0 ± 1.4	1.0 ± 0.0	3.0 ± 2.4	3.0 ± 2.4
$Norm_{KK} = \frac{n_{KK}}{r_{KK}}$	$\mathbf{0.5 \pm 0.5}$	$\mathbf{1.0 \pm 1.0}$	$\mathbf{0.33 \pm 0.33}$	$\mathbf{0.33 \pm 0.33}$
$n_{Kpi}:\ B4TRS \cdot B4CCD$	1.0 ± 1.0	1.0 ± 1.0	1.0 ± 1.0	1.0 ± 1.0
$r_{Kpi}:\ TG \cdot TGKIN \cdot TGPV$	10.0 ± 9.5	2.0 ± 1.4	11.0 ± 10.5	11.0 ± 10.5
$Norm_{Kpi} = \frac{n_{Kpi}}{r_{Kpi}}$	$\mathbf{0.10 \pm 0.10}$	$\mathbf{0.50 \pm 0.50}$	$\mathbf{0.091 \pm 0.091}$	$\mathbf{0.091 \pm 0.09}$

Table 9: **PNN2 2-Beam Normalization**. The 2-BM Normalization has 2 branches that are further bifurcated as seen in Figure 5(b). The normalization results are in the $Norm_{KK,Kpi}$ rows.

$2-BMBackground$ ($\times 10^{-3}$)	$\leq run$ 49151 *delc, delc-3*	$\leq run$ 49151 *delc-6*	$> run$ 49151 *delc*	All Runs *delc, delc-3*	All Runs *delc-6*
N_{Kpi} measured	$\mathbf{0.561 \pm 0.561}$	$\mathbf{0.565 \pm 0.565}$	117.83 ± 147.24	1.64 ± 1.64	1.65 ± 1.65
N_{Kpi} scaled by PNN1	———	———	$< 1^{st} half$	———	———
N_{Kpi} scaled by KB_{live}	———	———	$\mathbf{0.863 \pm 0.863}$	$\mathbf{1.42 \pm 1.42}$	$\mathbf{1.43 \pm 1.43}$

Table 10: **PNN2 Kpi Background.** Scaled to the 3/3 sample and the PV acceptance correction has been applied. Calculations for the *All Runs-delc* sample are shown in equations 5-12. Scaling factor of KB_{Live} is 1.54. Results for other sample are made in the same fashion. Background for $> run$ 49151-*delc-6*$= 0.870 \pm 0.870$.

Equations 5 thru 12 use measurements from the PNN2-*delc* sample which accepts PNN1 or PNN2 triggers and define $DELCO = delc$. The factor of 3 is to scale the 1/3 data sample to the 3/3 sample. $\frac{A_{PV_{pnn2}}}{A_{PV_{beam}}}$ is the PV acceptance correction.

$$N_{2-bmbkg} = \left(3 \cdot \frac{A_{PV_{pnn2}}}{A_{PV_{beam}}}\right) \cdot (N_{KK} + N_{Kpi}) \tag{5}$$

We do not directly measure N_{Kpi}, so we must expand N_{Kpi},

$$N_{2-bmbkg} = \left(3 \cdot \frac{A_{PV_{pnn2}}}{A_{PV_{beam}}}\right) \cdot \Big(N_{KK} + \big(N_{Kpi_{early}} + (f_{KB_{Live}} \cdot N_{Kpi_{early}})\big)\Big) \tag{6}$$

Substitute measurable quantities for N_{KK} and N_{Kpi}.

$$N_{2-bmbkg} = \left(3 \cdot \frac{A_{PV_{pnn2}}}{A_{PV_{beam}}}\right) \cdot \left(\frac{Norm_{KK}}{R_{KK} - 1} + (1 + f_{KB_{Live}}) \cdot \frac{Norm_{Kpi}}{R_{Kpi} - 1}\right) \tag{7}$$

Place measured quantities, from Tables 8 and 9, into equation.

$$N_{2-bmbkg} = \left(3 \cdot \frac{0.60}{0.95}\right) \cdot \left(\frac{\frac{1}{3.}}{63.7 - 1} + (1 + 1.54) \cdot \frac{\frac{1}{10.}}{339.0 - 1}\right) \tag{8}$$

$$N_{2-bmbkg} = \left(3 \cdot \frac{0.60}{0.95}\right) \cdot (.00532 + (1 + 1.54) \cdot 0.000296) \tag{9}$$

Determine the *early runs* and *late runs* background values.

$$N_{2-bmbkg} = (.00101) + (0.000561\ (early) + 0.000863\ (late)) \tag{10}$$

Evaluate and obtain a value for N_{KK} (first quantity) and N_{Kpi} (second quantity).

$$N_{2-bmbkg} = 0.0101 + 0.00142 \tag{11}$$

Now obtain the total 2-beam background value.

$$N_{2-bmbkg} = 0.0115 \pm 0.0115 \tag{12}$$

4 Total Beam Background Estimate

A PV acceptance correction of $\frac{0.6}{0.95}$ has been applied to the 1 and 2 beam results shown in Table 11. This table also compares the current results to what was observed in E949-PNN1 analysis, as reported in the K034 technote, and E787-PNN2 analysis, as reported in Bipul's Thesis. After scaling, the total beam-background is $\mathbf{0.0117 \pm 0.0117}$.

Possible differences between this reported background and the final background PNN2 will use are the following:

- *ccdpul* work is continuing now. Improvements in this cut could have a noticeable effect on this result.
- The $PV_{Acceptance}$ has not been evaluated.

When the cuts are frozen and the 3/3 processing completes, we will absorb and needed changes. However, the 1/3 result should not change significantly from what is reported here. The final conclusion is that the beam background is small.

Background ($\times 10^{-3}$)	E949-PNN1	E787-PNN2	PNN2 (1/3)	
DELCO	*delc*	*delc-6*	*delc*, *delc-3*	*delc-6*
1-BM	3.86 ± 2.36	1.66 ± 1.66	0.418 ± 0.418	0.418 ± 0.418
2-BM KK	0.983 ± 0.983	145.9 ± 145.9	10.1 ± 10.1	9.82 ± 9.82
2-BM Kpi	0.106 ± 0.106	19.7 ± 19.7	1.42 ± 1.42	1.43 ± 1.43
2-BM	1.14 ± 1.14	165.6 ± 165.6	11.5 ± 11.5	11.3 ± 11.3
$Total$ (1BM+2BM)	5.00 ± 2.62	167.3 ± 167.3	$\mathbf{11.9 \pm 11.9}$	$\mathbf{11.7 \pm 11.7}$

Table 11: **Total Background Comparison.** Values in PNN2 (1/3) column are calculated as seen in equations 1 - 4 and equations 5 - 12. The errors are statistical. E949-PNN1 column is the results reported in the K034 technote 1/3 sample. E787-PNN2 is the results reported in Bipul's Thesis for the 1/3 sample. KB_{live} for PNN1 is 1.77×10^{12} and for E787 is 1.71×10^{12} . E787 background has been scaled up accordingly for comparison purposes.

Background ($\times 10^{-3}$)	PNN2 (1/3)			
DELCO	*delc*, *delc-3*		*delc-6*	
Kinematic Box	*box787*	*box949*	*box787*	*box949*
1-BM			0.418 ± 0.418	0.418 ± 0.418
2-BM KK			10.1 ± 10.1	9.82 ± 9.82
2-BM Kpi			1.42 ± 1.42	1.43 ± 1.43
2-BM			11.5 ± 11.5	11.3 ± 11.3
$Total$ (1BM+2BM)			$\mathbf{11.9 \pm 11.9}$	$\mathbf{11.7 \pm 11.7}$

Table 12: **Total Background.** Values in PNN2 (1/3) column are calculated as seen in equations 1 - 4 and equations 5 - 12. The errors are statistical.

5 Conclusions

The beam background has been reduced compared to E787-PNN2 results. We expect about ~ 3 times the background in the PNN2 box compared to the PNN1 box due to phase space. The results are consistent with that expectation.

Items that need further investigation or implementation of safety cuts:

- The need to create a cut to remove KIC-like events, as observed in the KK rejection branch.
- A beam particle entering TG after the initial Kaon and before *trs*.
- *b4ccd.function* should be reexamined.

6 Appendix A

This note uses summary tables which were extracted from a set of detailed tables. These detailed tables show every cut used in every bifurcation. These tables are available here:

- PNN1 tables
- PNN2 tables

For posterity and ability to recreate what was reported in this technote, tarred-gzipped files are stored for all sets of data that are reported in this note. The files included are all cut functions, histograms, scripts, raw generated latex files, and much much more. These are available here:

- PNN1

  Early runs:

  Late runs:

  All runs:

- PNN2

  Early runs:

  Late runs:

  All runs: